Synthesis of $[Ru_2(CO)_5\{1,2\text{-bis}(\mu\text{-alkylamido})\text{-}1,2\text{-bis}(2\text{-pyridyl})\text{ethane}\}]$ and $[Ru_2(CO)_4\{\text{pyridine-2-carbaldehyde } N\text{-alkylimine}\}_2]$ and the Molecular Structure of Bis(pyridine-2-carbaldehyde *N*-isopropylimine)-tetracarbonyldiruthenium. Unprecedented CO-Induced Carbon–Carbon Bond Formation between Two Pyridine-2-carbaldimines in Dinuclear Ruthenium Carbonyl Complexes

Louis H. Polm, Cornelis J. Elsevier, Gerard van Koten, Jan M. Ernsting, Derk J. Stufkens, and Kees Vrieze*

Anorganisch Chemisch Laboratorium, University of Amsterdam, Nieuwe Achtergracht 166, 1018 WV Amsterdam, The Netherlands

Ronald R. Andrêa and Casper H. Stam

Laboratorium voor Kristallografie, University of Amsterdam, Nieuwe Achtergracht 166, 1018 WV Amsterdam, The Netherlands

Received September 4, 1986

Reaction of either $Ru_2(CO)_6$(R-Pyca{R^1,R^2}) with R-Pyca{R^1,R^2} (R-Pyca{R^1,R^2} = 6-$R^1C_5H_3N$-2-C(R^2)=NR; R = *t*-Bu, *i*-Pr, c-Hex; R^1 = Me, H; R^2 = H) or $Ru_3(CO)_{12}$ with R-Pyca{R^1,R^2} at 110 °C in toluene yields $Ru_2(CO)_5$(R-APE{R^1,R^2}) (R-APE{R^1,R^2} = [6-$R^1C_5H_3N$-2]C(R^2)(NR)C(R^2)(NR)[2-C_5H_3N-6-R^1]). The 10e donor ligand R-APE{R^1,R^2} arises from the carbon–carbon coupling of two R-Pyca{R^1,R^2} molecules. The product obtained after heating a xylene solution of either $Ru_2(CO)_5$(R-APE{R^1,R^2}) or $Ru_3(CO)_{12}$ with R-Pyca{R^1,R^2} at 140 °C depends strongly on the substituent R^1 at the 6-position of the pyridine ring. In the case that R^1 = Me, one CO ligand per molecule is evolved and $Ru_2(CO)_4$(R-APE{Me,H}) possessing a 10e R-APE ligand and a Ru–Ru bond is obtained. However, when R^1 = H, $Ru_2(CO)_4$(R-Pyca)$_2$ is formed exclusively, as a result of CO elimination, selective carbon–carbon bond rupture, and breaking of the metal–metal bond. The structure of $Ru_2(CO)_4$(*i*-Pr-Pyca)$_2$ was solved by X-ray structure determination. Crystals of $C_{22}H_{22}N_4O_2Ru_2$ are monoclinic of space group $P2_1/a$ with cell constants a = 10.976 (2) Å, b = 12.936 (2) Å, c = 8.881 (1) Å, β = 113.78 (1)°, and Z = 2. A total of 1514 reflections have been used in the refinement, which resulted in a final R value of 0.030 (R_w = 0.055). The Ru–Ru distance is 3.30 (1) Å. The molecule contains four terminal CO's and two *i*-Pr-Pyca ligands coordinated in the σ-N, μ_2-N′, η^2-C=N′ (6e) mode to the $Ru_2(CO)_4$ core. The torsion angle of 6° between the C(1)–N(1) and C(2)–N(2) bonds indicates that the planarity of the N=CC=N system of free R-Pyca is not affected much upon coordination. $Ru_2(CO)_5$(*i*-Pr-APE{R^1,R^2}) is formed efficiently by reaction of $Ru_2(CO)_4$(*i*-Pr-APE{Me,H}) or $Ru_2(CO)_4$(*i*-Pr-Pyca)$_2$ with CO gas (1 atm) in toluene at 110 °C. These reverse reactions imply addition of CO in the case of $Ru_2(CO)_4$(*i*-Pr-APE{Me,H}) and addition of CO concomitant with the formation of a carbon–carbon bond between the two imine carbon atoms of the two R-Pyca's in the case of $Ru_2(CO)_4$(*i*-Pr-Pyca)$_2$. The latter reaction is unprecedented. Possible mechanisms for the formation of $Ru_2(CO)_5$(R-APE{R^1,R^2}) from $Ru_2(CO)_6$(R-Pyca{R^1,R^2}) and for the reversible carbon–carbon bond formation/bond rupture reaction, $Ru_2(CO)_4$(R-Pyca)$_2$ + CO ⇌ $Ru_2(CO)_5$(R-APE), are discussed.

Introduction

In a previous publication[1] we have shown that $Ru_2(CO)_6$(R-DAB) (R-DAB = RN=CHHC=NR)[2] containing a 6e donor σ-N, μ_2-N′, η^2-C=N′ bonded R-DAB ligand may react with free R-DAB to give $Ru_2(CO)_5$(IAE) (IAE = 1,2-bis(alkylamino)-1,2-bis(alkylimino)ethane;[2] the C–C coupled dimer of R-DAB) for R = *t*-Bu, *i*-Pr, and c-Hex. Extensive investigations of $Ru_2(CO)_5$(IAE) and comparison of its structure with that of $Mo_2(CO)_6$(IAE)[3] showed that the 10e donor IAE ligand consists of two R-DAB ligands connected by a C–C bond (Scheme I). It was shown conclusively by study of R-DAB ligands, which were substituted at one of the imino C atoms, that the C–C coupling takes place at the C atom of the formerly η^2-C=N bonded imine moiety.[1] Subsequent heating of $Ru_2(CO)_5$(IAE), containing a bridging CO group and no metal–metal bond, produced $Ru_2(CO)_4$(IAE) (R = *i*-Pr, c-Hex) having only terminal CO groups and a single Ru–Ru bond. Of great interest is that the C-C bond in $Ru_2(CO)_4$(IAE) could be

(1) Staal, L. H.; Polm, L. H.; Balk, R. W.; van Koten, G.; Vrieze, K.; Brouwers A. M. F. *Inorg. Chem.* **1980**, *19*, 3343.

(2) The relevant abbreviations used throughout this text are as follows. 1,4-Diaza-1,3-butadienes of formula RN=C(H)C(H)=NR are abbreviated to R-DAB. The pyridinecarbaldehyde imines of formula 6-$R^1C_5H_3N$-2-[C(R^2)=NR] are abbreviated to R-Pyca{R^1,R^2}; in the case that R^1 = R^2 = H it will be shortened to R-Pyca. R-IAE stands for 1,2-bis(alkylamino)-1,2-bis(alkylimino)ethane, RN=C(H)(H)C(NR)(H)-C(NR)C(H)=NR, the C–C coupled dimer of R-DAB. The 1,2-bis(alkylamido)-1,2-bis(2-pyridyl)ethane [6-$R^1C_5H_3N$-2]C(R^2)NR)C(R^2)NR)[2-C_5H_3N-6-R^1], the C–C coupled dimer of R-Pyca{R^1,R^2}, will be abbreviated to R-APE{R^1,R^2}; in the case that R^1 = R^2 = H it will be shortened to R-APE.

(3) Staal, L. H.; Oskam, A.; Vrieze, K.; Roosendaal, E.; Schenk, H. *Inorg. Chem.* **1979**, *18*, 1634.

0276-7333/87/2306-1096$01.50/0

Scheme I

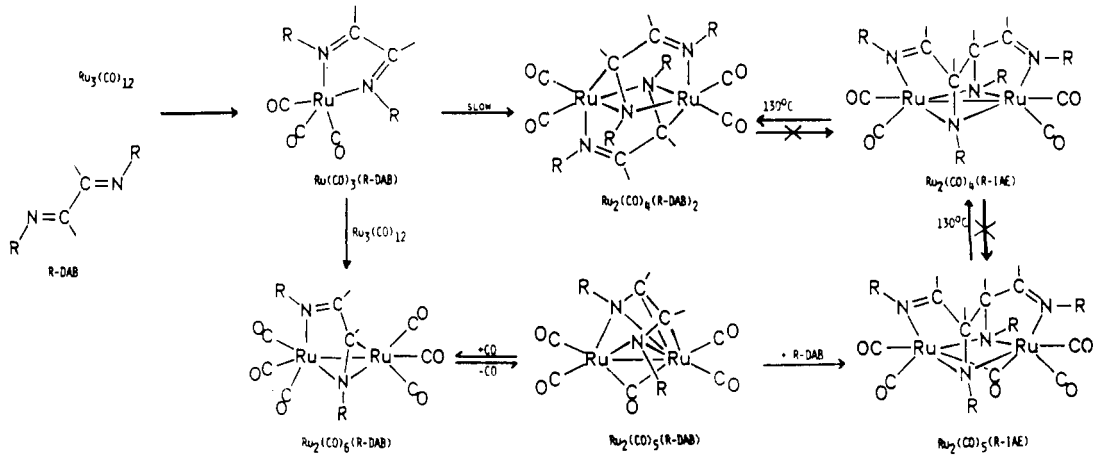

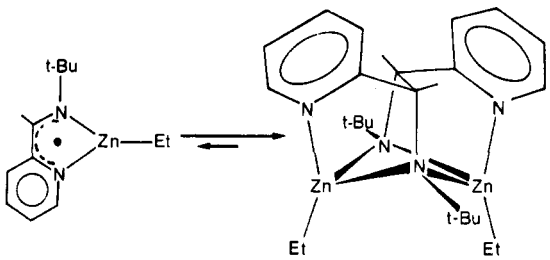

Figure 1. Equilibrium between the radical [ZnEt(*t*-Bu-Pyca)]• and its C–C coupled dimer [Zn_2Et_2(*t*-Bu-APE)].

ruptured again by heating the compound in xylene at 120 °C which gave isomeric $Ru_2(CO)_4$(R-DAB)$_2$ (R = *i*-Pr, c-Hex); for R = aryl this complex was formed directly from $Ru_3(CO)_{12}$ and aryl-DAB). The molecular structure of $Ru_2(CO)_4$(R-DAB)$_2$ (see Scheme I) consists of two σ-N, μ_2-N′, η^2-C=N′ 6e donor R-DAB ligands at both sides of the $Ru_2(CO)_4$ core.[1] Furthermore, it has been shown (see Scheme I) that there is an intermediate compound, $Ru_2(CO)_5$(R-DAB) (R = *i*-Pr, c-Hex, *t*-Bu), containing, as shown by an X-ray structural determination of $Ru_2(CO)_5$(*i*-Pr-DAB),[4] a σ-N, σ-N′, η^2-C=N, η^2-C′=N′ bonded R-DAB ligand, which donates eight electrons to the $Ru_2(CO)_5$ skeleton and which possesses both a bridging CO group and a Ru–Ru single bond.

Recently a rationale has been proposed for the insertion reaction of R-DAB into the Ru–C bond of $Ru_2(CO)_5$(R-DAB).[4] In this context it is of interest to point out that the C–C coupled ligand can also be prepared by the dimerization reaction of two persistent [EtZn(R-Pyca)]• radicals to give Et_2Zn_2(R-APE)[5] (see Figure 1). The structural details of [Et_2Zn_2(R-APE)] (R-APE = 1,2-bis-(μ-alkylamido)-1,2-bis(2-pyridyl)ethane)[2] show that the structure comprises two C–C coupled R-Pyca ligands and is very similar indeed to, for example, $Mo_2(CO)_6$(R-IAE).[3]

In view of our earlier studies involving R-DAB systems, attention has been focussed on the preparation and reactions of analogous pyridine-2-carbaldehyde *N*-alkylimine ruthenium carbonyl complexes, in order to study (i) the possibility of C—C bond formation and C—C bond rupture reactions between these ligands and (ii) the influence of the incorporation of one C=N bond of the N=CC=N system in a pyridine ring on these reactions as well as (iii) the effect of a 6-Me substituent in the pyridine ring may exert on the relative stability of intermediates formed in the reactions of R-Pyca with $Ru_3(CO)_{12}$. The results of this study, comprising in particular the observation of a novel, reversible CO-induced C–C bond formation/bond rupture reaction and the molecular structure of $Ru_2(CO)_4$(*i*-Pr-Pyca)$_2$, one of the C–C decoupling products, will be discussed in this paper.

Experimental Section

Materials and Apparatus. NMR spectra were recorded on a Bruker WM 250 spectrometer (^{1}H) and on a Bruker WP 80 apparatus (^{13}C). IR spectra were measured with a Perkin-Elmer 283 spectrophotometer and a Nicolet 7199B interferometer provided with a liquid-nitrogen-cooled HgCdTe detector. Mass spectra were obtained with a Varian MAT 711 mass spectrometer applying the Field Desorption technique.[6]

Elemental analyses were carried out by the Section Elemental Analysis of the Institute for Applied Chemistry, TNO, Zeist, The Netherlands. All preparations were carried out in an atmosphere of purified nitrogen, using carefully dried solvents. Silica gel for column chromatography (60 mesh) was dried and activated before use. $Ru_3(CO)_{12}$ was purchased from Strem Chemicals (USA) and was used without purification. The pyridine-2-carbaldehyde imine ligands R-Pyca{R^1,R^2} were prepared according to standard methods.[7]

Synthetic Aspects. Syntheses of $Ru_2(CO)_5$(R-APE) [R = *t*-Bu (1a), *i*-Pr (1b), c-Hex (1c)]. A solution of $Ru_2(CO)_6$(R-Pyca) (0.5 mmol), prepared according to ref 8, and R-Pyca (0.5 mmol) in 50 mL of toluene was refluxed during 3 h, after which the toluene was evaporated. The crude product was washed with *n*-hexane to remove traces of unreacted $Ru_2(CO)_6$(R-Pyca) and then further purified by column chromatography on a silica gel column using CH_2Cl_2 as the eluent. The pure products were precipitated by adding *n*-pentane to the CH_2Cl_2 solution of the complexes and filtered off. After being dried under vacuum (0.05 mmHg) for 1 h, the complex was obtained as an orange powder in ca. 75% yield (0.35–0.4 mmol). Recrystallization of this powder from a CH_2Cl_2/diethyl ether mixture, 1/1 (v/v), afforded a crystalline orange-red product. Alternatively, the same procedure could be followed, using $Ru_3(CO)_{12}$ (0.33 mmol) and R-Pyca{H,H} (1.0 mmol). The yield of **1a–c** was then ca. 70%.

Syntheses of $Ru_2(CO)_5$(R-APE{Me,H}) [R = *t*-Bu (1d), *i*-Pr (1e), c-Hex (1f)]. The same procedure was followed as in the case of the $Ru_2(CO)_5$(R-APE{H,H}) complexes, using $Ru_2(CO)_6$-(R-Pyca{Me,H}) and R-Pyca{Me,H}. When the alternative procedure, using $Ru_3(CO)_{12}$ and R-Pyca{Me,H}, was applied, a mixture

(4) Keijsper, J.; Polm, L. H.; van Koten, G.; Vrieze, K.; Abbel, G.; Stam, C. H. *Inorg. Chem.* **1984**, *23*, 2142.
(5) van Koten, G.; Jastrzebski, J. T. B. H.; Vrieze, K. *J. Organomet. Chem.* **1983**, *250*, 49.
(6) (a) Mann, B. E. *Adv. Organomet. Chem.* **1974**, *12*, 135. (b) Jolly, P. W.; Myott, R. *Adv. Organomet. Chem.* **1980**, *19*, 257. (c) Staal, L. H.; van Koten, G.; Fokkens, R. H.; Nibbering, N. M. M. *Inorg. Chim. Acta* **1981**, *50*, 205.
(7) (a) Bähr, G.; Thämlitz, H. *Z. Anorg. Allg. Chem.* **1955**, *282*, 3. (b) Bähr, G.; Döge, H. G. *Z. Anorg. Allg. Chem.* **1957**, *292*, 119. (c) Robinson, M. A.; Curry, J. D.; Busch, D. H. *Inorg. Chem.* **1963**, *6*, 1178.
(8) Polm, L. H.; van Koten, G.; Elsevier, C. J.; Vrieze, K.; van Santen, B. F. K.; Stam, C. H. *J. Organomet. Chem.* **1986**, *304*, 353.

of products was obtained. As shown by the IR and ^1H NMR spectra, this crude reaction product consisted of $Ru_2(CO)_5$(R-APE{Me,H}) (80–90%) and $Ru_2(CO)_4$(R-Pyca{Me,H})$_2$ (10–20%). Workup was accomplished as described above, yielding $Ru_2(CO)_5$(R-APE{Me,H}) (**1d–f**) in 55–60% yield.

Syntheses of $Ru_2(CO)_4$(R-Pyca)$_2$ [R = *t*-Bu (2a), *i*-Pr (2b), c-Hex (2c)]. A solution of $Ru_3(CO)_{12}$ (0.33 mmol) and R-Pyca (1.0 mmol) or of $Ru_2(CO)_6$(R-Pyca) (0.5 mmol) and R-Pyca{H,H} (0.5 mmol) in 50 mL of xylene was refluxed for 18 h. When the solution was cooled to room temperature, the product precipitated as a yellow powder. Complexes **2a–c** were obtained as pure pale yellow powders in 50–60% yield (0.25–0.3 mmol) by filtration and successive washing with dichloromethane (3 × 10 mL). Alternatively, these compounds could be obtained by refluxing the appropriate complex $Ru_2(CO)_5$(R-APE) (**1a–c**) in xylene for 18–20 h, followed by the same workup procedure as described above. The yields of $Ru_2(CO)_4$(R-Pyca)$_2$ (**2a–c**) were slightly higher (60–70%, 0.3–0.35 mmol). Single crystals of **2b**, which were suitable sized for an X-ray diffraction study, could be obtained by recrystallization from a dichloromethane solution at +4 °C.

Syntheses of $Ru_2(CO)_4$(R-APE{Me,H}) [R = *t*-Bu (3a), *i*-Pr (3b), c-Hex (3c)]. A solution of $Ru_3(CO)_{12}$ (0.33 mmol) and R-Pyca{Me,H} (1.0 mmol) in 50 mL of xylene was refluxed for either 8 (in the case of **3a**[9]) or 16 h (for **3b** and **3c**). The xylene was evaporated in vacuo, and the residue, dissolved in a minimum volume of CH_2Cl_2, was purified on a silica gel column using diethyl ether/dichloromethane, 4/1 (v/v), as the eluent. The solvent of this column fraction was removed in vacuo, and the residue was recrystallized from diethyl ether. Complexes **3a–c** were obtained as ochreous, microcrystalline solids in about 60% yield (0.3 mmol).

These compounds could be prepared equally starting from $Ru_2(CO)_5$R-APE{Me,H}) **1d–f** by heating 0.3 mmol of the latter complex in 50 mL of xylene at reflux for 8 (**3a**) or 16 h (**3b,c**). Workup was carried out as described above; yield ca. 70% (0.2 mmol).

Synthesis of $Ru_2(CO)_4$(*t*-Bu-Pyca{Me,H})$_2$ (2d). A solution of $Ru_3(CO)_{12}$ (0.33 mmol) and *t*-Bu-Pyca{Me,H} (1.0 mmol) in 50 mL of xylene was refluxed for 20 h. The precipitated solid was filtered off and washed twice with 10 mL of dichloromethane, providing a yellow powder. The yield of this product, identified as **2d**, amounted to ca. 30%. The remainder (ca. 60%) was still dissolved in the xylene and consisted mainly of $Ru_2(CO)_4$(*t*-Bu-APE{Me,H}) (**3a**).

Synthesis of $Ru_2(CO)_4$(*i*-Pr-Pyca{Me,H})$_2$ (2e). $Ru_2(CO)_4$(*i*-Pr-APE{Me,H}) (0.2 mmol) was heated at reflux in 30 mL of xylene for 70 h. After the solution was cooled to room temperature, the precipitated product was filtered on a G4 glass filter and washed with dichloromethane (2 × 10 mL). Complex **2e** was obtained as a pale yellow powder in <10% yield. The remainder mainly consisted of not identified decomposition products and starting materials.

Reaction of CO with $Ru_2(CO)_4$(*i*-Pr-Pyca)$_2$ (2b) and $Ru_2(CO)_4$(*i*-Pr-APE{Me,H}) (3b). At 100 °C CO gas was bubbled at a rate of about 50 mL/h via a small sintered inlet (5-mm G4 glass frit) through a toluene solution (30 mL) of $Ru_2(CO)_4$(*i*-Pr-Pyca)$_2$ (**2b**, 0.25 mmol) or $Ru_2(CO)_4$(*i*-Pr-APE{Me,H}) (**3b**, 0.3 mmol). Complete conversion into either $Ru_2(CO)_5$(*i*-Pr-APE) (**1b**) or $Ru_2(CO)_5$(*i*-Pr-APE{Me,H}) (**1e**) was obtained after 2 or 7 h, respectively, as was established by IR spectra (1650–2200 cm^{-1} region) of the reaction mixtures. When the toluene solutions of **2b** and **3b** were heated at 60 °C under CO pressure (20 bars) in a 250-mL autoclave, the conversions were complete in half an hour (**1b**) and 2 h (**1e**), respectively.

Crystal Structure Determination of $Ru_2(CO)_4$(*i*-Pr-Pyca)$_2$: Tetracarbonylbis(pyridine-2-carbaldehyde isopropylimine)diruthenium [$C_{22}H_{22}N_4O_4Ru_2$ (2b)]. Crystals of the title compound are monoclinic of space group $P2_1/a$ with two molecules in a unit cell of dimensions a = 10.976 (2) Å, b = 12.936 (2) Å, c = 8.881 (1) Å, β = 113.78 (1)°, V = 1153.9 (5) Å^3, d_{calcd} = 1.76g cm^{-3}, and Z = 2.

A total of 2057 intensities ($2.5 < \theta < 65°$) were measured on a Nonus CAD 4 diffractometer (scan method θ–2θ) at 25 °C employing graphite-monochromated Cu Kα radiation. Of these, 543 were below the $2.5\sigma(I)$ level and were treated as unobserved. In view of the small crystal size (μ = 111.6 cm^{-1}; crystal dimensions 0.05 × 0.05 × 0.08 mm) no absorption correction was applied. The structure was derived from a Patterson minimum function based on the four Ru positions in the unit cell. Block-diagonal least-squares refinement, anisotropic for Ru, C, N, and O and isotropic for H, resulted in a final R value of 0.030 for the 1514 observed reflections (R_w = 0.055).[10a] A final Fourier difference map showed

(9) After longer reaction times, a substantial amount of $Ru_2(CO)_4$(*t*-Bu-Pyca{Me,H})$_2$ was formed; see also "synthesis of **2d**".

Table I. Atomic Coordinates (Esd's in Parentheses)

Ru	0.41283 (3)	0.49193 (3)	0.61379 (4)
C(1)	0.4589 (5)	0.3799 (4)	0.3541 (7)
C(2)	0.3147 (5)	0.3864 (4)	0.2921 (6)
C(3)	0.2313 (7)	0.3618 (5)	0.1298 (7)
C(4)	0.0962 (6)	0.3666 (6)	0.0835 (8)
C(5)	0.0432 (6)	0.3981 (6)	0.1910 (9)
C(6)	0.1306 (6)	0.4235 (5)	0.3490 (7)
C(7)	0.2990 (6)	0.5732 (5)	0.6736 (7)
C(8)	0.4370 (6)	0.4160 (5)	0.8038 (7)
C(9)	0.6251 (6)	0.3126 (4)	0.6154 (7)
C(10)	0.5347 (7)	0.2214 (5)	0.6388 (7)
C(11)	0.7290 (6)	0.3498 (5)	0.7782 (8)
N(1)	0.5335 (4)	0.3978 (3)	0.5257 (5)
N(2)	0.2645 (4)	0.4192 (3)	0.4002 (6)
O(1)	0.2288 (5)	0.6174 (4)	0.7141 (9)
O(2)	0.4536 (5)	0.3765 (4)	0.9251 (5)
H(1)	0.485 (5)	0.320 (4)	0.314 (6)
H(3)	0.272 (6)	0.328 (4)	0.053 (7)
H(4)	0.031 (7)	0.354 (6)	−0.039 (9)
H(5)	−0.027 (7)	0.395 (6)	0.177 (9)
H(6)	0.098 (4)	0.449 (3)	0.423 (5)
H(9)	0.172 (5)	0.215 (4)	0.526 (6)
H(101)	0.013 (8)	0.256 (7)	0.756 (10)
H(102)	0.122 (10)	0.326 (7)	0.701 (12)
H(103)	−0.024 (7)	0.296 (6)	0.529 (8)
H(111)	0.279 (7)	0.211 (5)	0.840 (8)
H(112)	0.195 (9)	0.131 (7)	0.854 (10)
H(113)	0.292 (7)	0.101 (6)	0.770 (9)

Table II. Selected Bond Lengths (Å) (Esd's in Parentheses)

Ru–Ru*	3.303 (1)	N(1)–C(1)	1.428 (7)
Ru–N(1)	2.164 (5)	C(1)–C(2)	1.454 (7)
Ru–N(2)	2.155 (4)	C(2)–N(2)	1.354 (8)
Ru–N(1)*	2.123 (5)	C(2)–C(3)	1.397 (7)
Ru–C(1)*	2.119 (5)	C(3)–C(4)	1.371 (10)
Ru–C(7)	1.886 (7)	C(4)–C(5)	1.365 (12)
Ru–C(8)	1.877 (6)	C(5)–C(6)	1.383 (8)
		C(6)–N(2)	1.353 (8)
C(7)–O(1)	1.129 (10)	N(1)–C(9)	1.488 (6)
C(8)–O(2)	1.139 (8)	C(9)–C(10)	1.544 (9)
		C(9)–C(11)	1.514 (8)

Table III. Selected Bond Angles (deg) (Esd's in Parentheses)

N(2)–Ru–N(1)	78.0 (2)	Ru*–C(1)–N(1)	70.5 (3)
N(2)–Ru–N(1)*	93.9 (2)	Ru*–C(1)–C(2)	124.7 (4)
N(2)–Ru–C(1)*	133.3 (2)	N(1)–C(1)–C(2)	117.6 (6)
N(2)–Ru–C(7)	98.1 (2)	Ru–N(2)–C(2)	112.5 (3)
N(2)–Ru–C(8)	110.2 (2)	Ru–N(2)–C(6)	127.6 (4)
N(1)–Ru–C(7)	175.7 (2)	C(2)–N(2)–C(6)	118.2 (5)
N(1)–Ru–C(8)	98.4 (2)	C(1)–C(2)–N(2)	116.2 (4)
N(1)–Ru–C(1)*	91.1 (2)	C(1)–C(2)–C(3)	122.5 (6)
N(1)–Ru–N(1)*	79.2 (2)	N(2)–C(2)–C(3)	121.2 (5)
C(7)–Ru–C(8)	84.7 (3)		
C(7)–Ru–C(1)*	90.3 (3)	C(2)–C(3)–C(4)	118.6 (7)
C(7)–Ru–N(1)*	99.4 (2)	C(3)–C(4)–C(5)	121.2 (6)
C(8)–Ru–C(1)*	116.3 (2)	C(4)–C(5)–C(6)	117.6 (6)
C(8)–Ru–N(1)*	154.8 (2)	C(5)–C(6)–N(2)	123.1 (7)
C(1)*–Ru–N(1)*	39.4 (2)		
		Ru–C(7)–O(1)	176.0 (6)
Ru–N(1)–Ru*	100.8 (2)	Ru–C(8)–O(2)	175.0 (6)
Ru–N(1)–C(1)	107.8 (3)		
Ru*–N(1)–C(1)	70.2 (3)	N(1)–C(9)–C(10)	109.6 (5)
Ru–N(1)–C(9)	127.1 (4)	N(1)–C(9)–C(11)	111.2 (4)
Ru*–N(1)–C(9)	121.6 (4)	C(10)–C(9)–C(11)	111.6 (5)
C(1)–N(1)–C(9)	115.1 (4)		

Table IV. IR Absorption and FD Mass Spectrometric Data of $Ru_2(CO)_n$(R-APE) (n = 4, 5) and $Ru_2(CO)_4$(R-Pyca)$_2$

type of complex	substituents[a] R^1	R	M_r (M_r(calcd))[b]	IR ν(CO)/cm^{-1}[c]
$Ru_2(CO)_5$(R-APE{R^1,R^2})				
1a	H	*t*-Bu	667 (666.67)	2016, 1988, 1934, 1695
1b	H	*i*-Pr	638 (638.60)	2016, 1991, 1937, 1693
1c	H	c-Hex	719 (718.73)	2017, 1990, 1936, 1689
1d	Me	*t*-Bu	695 (694.71)	2019, 1990, 1937, 1698
1e	Me	*i*-Pr	668 (666.67)	2017, 1988, 1934, 1695
$Ru_2(CO)_4$(R-Pyca{R^1,R^2})$_2$				
2a	H	*t*-Bu	636 (638.65)	1969, 1899
2b	H	*i*-Pr	610 (610.59)	1972, 1904
2c	H[d]	c-Hex	691 (690.72)	1970, 1903
2d	Me[d]	*t*-Bu	668 (666.70)	1972, 1900
2e	Me[d]	*i*-Pr	640 (638.65)	1973, 1905
$Ru_2(CO)_4$(R-APE{R^1,R^2})				
3a	Me	*t*-Bu	668 (666.70)	1979, 1937, 1895
3b	Me	*i*-Pr	640 (638.65)	1977, 1937, 1894
3c	Me	c-Hex	717 (718.78)	1978, 1936, 1893

[a] R^2 = H in all cases. [b] Calculated values based on Ru isotope distribution. [c] Measured in dichloromethane solution. [d] Isolated in very low yield, see text.

Table V. ^{1}H NMR Data (250.1 MHz) of $Ru_2(CO)_n$(R-APE) (n = 4, 5) and $Ru_2(CO)_4$(R-Pyca)$_2$[a]

type of complex	ligand[b] R^1	R	pyridine ring substituents R^1 = H or Me	H_4	H_3	H_5	R^2 = H	substituents (R)
$Ru_2(CO)_5$(R-APE)[c]								
1a	H	*t*-Bu	8.46 (d)	7.80 (m)	7.48 (d)	7.29 (m)	3.94 (s)	1.01 (s)
1b	H	*i*-Pr	8.51 (d)	7.78 (m)	7.39 (d)	7.31 (m)	3.83 (s)	3.33 (sept, J = 6), 1.19 (d, J = 6), 0.72 (d, J = 6)
1c	H	c-Hex	8.51 (d)	7.78 (m)	7.37 (d)	7.30 (m)	3.82 (s)	2.89 (m), (2–0.6) (m)
1d	Me	*t*-Bu	2.69 (s)	7.64 (m)	7.25 (d)	7.15 (m)	3.95 (s)	1.03 (s)
1e	Me	*i*-Pr	2.64 (s)	7.63 (m)	7.19 (d)	7.16 (m)	3.76 (s)	3.27 (sept, J = 6), 1.16 (d, J = 6), 0.66 (d, J = 6)
1f	Me	c-Hex	2.71 (s)	7.62 (m)	7.18 (d)	7.18 (m)	3.81 (s)	2.71 (m), (2–0.5) (m)
$Ru_2(CO)_4$(R-Pyca)$_2$[d]								
2a	H	*t*-Bu	8.42 (d)	7.52 (m)	7.45 (d)	6.96 (m)	5.14 (s)	0.77 (s)
2b	H	*i*-Pr	8.38 (d)	7.51 (m)	7.41(d)	6.93 (m)	4.77 (s)	1.86 (sept, J = 6), 0.83 (d, J = 6), 0.10 (d, J = 6)
2c	H	c-Hex	8.40 (d)	7.50 (m)	7.43 (d)	6.96 (m)	4.81 (s)	1.96 (m), (1.5–0.5) (m)
2d	Me	*t*-Bu	2.69 (s)	7.44 (m)	7.31 (d)	6.98 (m)	5.19 (s)	0.77 (s)
2e	Me	*i*-Pr	2.69 (s)	7.45 (m)	7.32 (d)	6.99 (m)	4.84 (s)	1.87 (sept, J = 6), 0.84 (d, J = 6), 0.14 (d, J = 6)
$Ru_2(CO)_4$(R-APE)[d]								
3a	Me	*t*-Bu	2.82 (s)	7.60 (m)	7.10 (d)	7.00 (m)	4.10 (s)	0.97 (s)
3b	Me	*i*-Pr	2.83 (s)	7.60 (m)	7.17 (d)	7.11 (m)	3.97 (s)	3.79 (sept, J = 7), 0.74 (d, J = 7), 0.65 (d, J = 7)
3c	Me	c-Hex	2.83 (s)	7.59 (m)	7.08 (d)	7.08 (m)	3.96 (s)	3.25 (m), (1.6–0.7) (m)

[a] δ in parts per million downfield from internal Me_4Si (s, singlet; d, doublet; sept, septet; m, multiplet); J in Hz; measured at +30 °C. [b] R^2 = H in all cases. [c] Solvent CD_2Cl_2. [d] Solvent $CDCl_3$.

Table VI. ^{13}C NMR Data (20.1 MHz) of $Ru_2(CO)_n$(R-APE) (n = 4, 5) and $Ru_2(CO)_4$(R-Pyca)$_2$[a]

type of complex	ligand[b] R^1	R	pyridine ring carbon atom C_2	C_6	C_3	C_4	C_5	R^1 = Me	NC(H)	substituents (R)	M–CO
$Ru_2(CO)_5$(R-APE)[c]											
1a	H	*t*-Bu	166.6	151.2	139.1	123.5	120.9		74.5	59.2, 32.7	202.4, 201.7
1b	H	*i*-Pr	165.6	152.3	139.0	123.1	121.1		72.0	59.6, 25.5, 25.1	202.1
1c	H	c-Hex	163.6	151.1	138.1	122.5	119.7		70.1	71.5, 34.3, 25.7, 25.3	201.2, 200.7
1d	Me	*t*-Bu	166.1	159.4	138.3	122.8	117.7	26.2	74.2	59.1, 33.4	202.1, 201.7
1e	Me	*i*-Pr	166.0	160.9	138.4	123.6	118.3	26.5	72.8	59.2, 25.3	203.1, 201.8
1f	Me[e]	c-Hex									201.6
$Ru_2(CO)_4$(R-APE)[d]											
3a	Me	*t*-Bu	173.1	159.0	136.4	119.2	118.4	28.2	61.6	60.3, 30.3	
3b	Me	*i*-Pr	173.8	160.9	137.5	122.0	117.3	28.5	68.4	62.5, 23.3, 21.6	209.8, 208.5
3c	Me	c-Hex	173.8	160.9	137.3	121.9	117.1	28.6	69.6	71.7, 35.0, 25.9, 25.7	

[a] δ in parts per million downfield from internal Me_4Si; measured at +30 °C. [b] R^2 = H in all cases. [c] Solvent CD_2Cl_2. [d] Solvent $CDCl_3$. [e] Not measured.

no residual density exceeding ±0.4 e/Å^3. A weighting scheme, $w = 1/(3 + F_o + 0.045F_o^2)$, was applied. The anomalous scattering of Ru was taken into account, and an extinction correction was included in the refinement.[10b] The molecular geometry of $Ru_2(CO)_4$(*i*-Pr-Pyca)$_2$ with the numbering of the atoms is shown in the PLUTO[10c] drawing of Figure 2, which also provides an ORTEP[10d] view of the molecule. Positional parameters of all atoms are given in Table I, and selected bond distances and angles are compiled in Tables II and III. Tables of all bond distances and angles as well as of observed and calculated structure factors and thermal parameters are included in the supplementary material.

Analytical Data. Elemental analysis of all complexes gave satisfactory results (see supplementary material). The complexes

(10) (a) $R = (\sum||F_o| - |F_c||)/\sum|F_o|$; $R_w = (\sum w||F_o| - |F_c||)/\sum w|F_o|$. (b) *International Tables for Crystallography*; Kynoch Press: Birmingham, England, 1974; Vol. IV. (c) Motherwell, S.; Clegg, B. PLUTO, Program for Plotting Molecular and Crystal Structures; University of Cambridge: Cambridge, England, 1978. (d) Johnson, C. K. ORTEP II, Report ORNL-5138; Oak Ridge National Laboratory: Oak Ridge, TN, 1976.

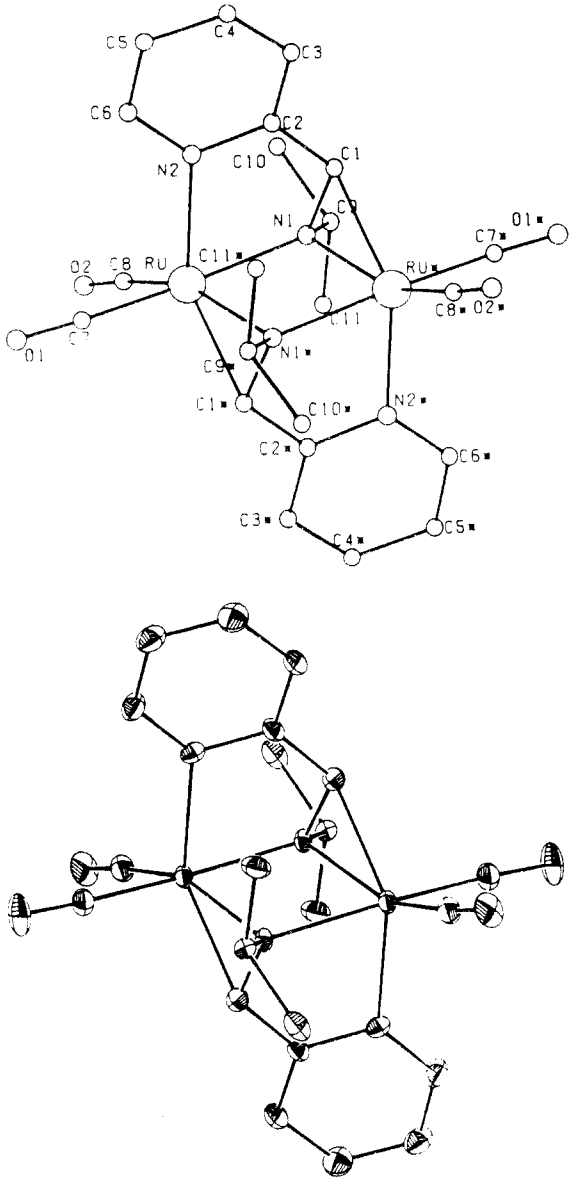

Figure 2. PLUTO and ORTEP representations of the molecular structure of $Ru_2(CO)_4(i\text{-Pr-Pyca})_2$ (**2b**) with the adopted numbering scheme.

showed characteristic IR ν(CO) absorptions, which are listed in Table IV. Mass spectra were recorded by using the field desorption technique.[6] Correct m/z values for the molecular ions were obtained, which showed the expected isotope patterns. Observed and calculated m/z values are also listed in Table IV. ^1H and ^{13}C NMR data of the complexes are given in the Tables V and VI and are in agreement with the proposed structures of the various ruthenium complexes.

Results and Discussion

Molecular Structure of $Ru_2(CO)_4(i\text{-Pr-Pyca})_2$. A PLUTO and an ORTEP representation of the molecule are shown in Figure 2. The ruthenium atoms possess a distorted octahedral coordination geometry. The Ru–Ru intermetallic separation amounts to 3.30 (1) Å (Table II), which points to the absence of a metal–metal bond. The ruthenium atoms are bridged by two μ_2-N(1) and μ_2-N(1)* bonded imine fragments of the two *i*-Pr-Pyca ligands. The Ru–N(1) and Ru–N(1)* distances are 2.164 (5) and 2.123 (5) Å, respectively; the Ru-N(2) distance is 2.155 (4) Å, while the Ru–C(1)* distance in the C(1)*–N(1)* bridge amounts to 2.119 (5) Å. These are normal values for such bonds. From these observations it appears that the C(1)–C(1)* bond of $Ru_2(CO)_5$(i-Pr-APE) (see Figure 4), the

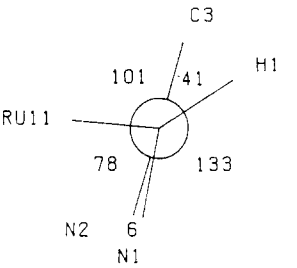

Figure 3. Newman projection of $Ru_2(CO)_4(i\text{-Pr-Pyca})_2$ (**2b**) viewed along the C(1)–C(2) axis.

progenitor of $Ru_2(CO)_4(i\text{-Pr-Pyca})_2$, has been broken. Furthermore it can be inferred that the two Pyca ligands are both coordinated in the σ-N, μ_2-N′, η^2-C=N′ (6e) bonding mode to the ruthenium atoms.

The C(1)—N(1) bond of 1.43 Å is significantly elongated compared to the C=N bond in uncoordinated R-DAB (1.26 Å)[11] and R-Pyca, as is expected for the η^2-bonding mode of this fragment.[12] The C(2)–N(2) distance of 1.35 (1) Å in the σ-N-coordinated pyridine ring is slightly larger than the comparable distance of 1.30 (1) Å in the σ-N-coordinated imine group in $Ru_2(CO)_4(i\text{-Pr-DAB})_2$,[1] which can be attributed to effective delocalization of electron density in the pyridine ring of the former complex. The bond distances within the pyridine ring are in the range of the normally observed values.

The N(1)–C(1)–C(2)–N(2) atoms almost form a plane, as can be inferred from the Newman projection shown in Figure 3, with a torsion angle of 6° between the C(1)–N(1) and C(2)–N(2) bonds. This implies that the planarity of the N=CC=N system in free Pyca ligands is not affected much by σ-N, μ_2-N′, η^2-C=N′ coordination, as was also observed for the R-DAB ligands in $Ru_2(CO)_4(i\text{-Pr-DAB})_2$ and $Fe_2(CO)_6$(c-Hex-DAB),[13] where angles of 6° and 12°, respectively, were found.

Syntheses. The thermal reactions in toluene of either $Ru_3(CO)_{12}$ with 3 molar equiv of R-Pyca or $Ru_2(CO)_6$(R-Pyca{R^1,R^2})[8] with 1 molar equiv of R-Pyca{R^1,R^2} give rise to the formation of the novel complexes $Ru_2(CO)_5$(R-APE{R^1,R^2}) (**1a–f**) (see eq 1 and 2 and Scheme II). These

$$^2/_3Ru_3(CO)_{12} + 2\ \text{R-Pyca}'\{R^1,R^{2\prime}\} \xrightarrow[\text{reflux, 3 h}]{\text{toluene}} Ru_2(CO)_5(\text{R-APE}\{R^1,R^2\}) + 3CO \quad (1)$$

$$Ru_2(CO)_6(\text{R-Pyca}\{R^1,R^2\}) + \text{R-Pyca}\{R^1,R^2\} \xrightarrow[\text{reflux, 3 h}]{\text{toluene}} Ru_2(CO)_5(\text{R-APE}\{R^1,R^2\}) + CO \quad (2)$$

compounds have been identified according to their stoichiometric composition inferred from elemental analysis and combined spectral data (Tables IV–VI). Furthermore, an X-ray study has been carried out for the representative example $Ru_2(CO)_5(i\text{-Pr-APE})$ (**1b**).[8] The yield of $Ru_2(CO)_5$(R-APE{R^1,R^2}) varied slightly with the nature of the alkyl group in the alkyl-Pyca ligands, whereas, in most cases, for aryl-Pyca no well-identified products could be obtained. In one experiment, $Ru_2(CO)_5(p\text{-tolyl-APE})$ could be isolated, although in very low yield (<5%). The observation that, generally, no $Ru_2(CO)_5$(aryl-APE) could be isolated is in qualitative agreement with previous results of Staal et al.[1] for the reaction of $Ru_3(CO)_{12}$ with *p*-

(11) (a) Staal, L. H.; van Koten, G.; Vrieze, K. *J. Organomet. Chem.* **1981**, *206*, 99. (b) Keijsper, J.; van der Poel, H.; Polm, L. H.; van Koten, G.; Vrieze, K.; Seignette, P. F. A. B.; Varenhorst, R.; Stam, C. H. *Polyhedron* **1983**, *2*, 1111.

(12) Vrieze, K.; van Koten, G. *Inorg. Chim. Acta* **1985**, *100*, 79.

(13) Frühauf, H.-W.; Landers, A.; Goddard, R.; Krüger, C. *Angew. Chem.* **1978**, *90*, 56.

Scheme II[a]

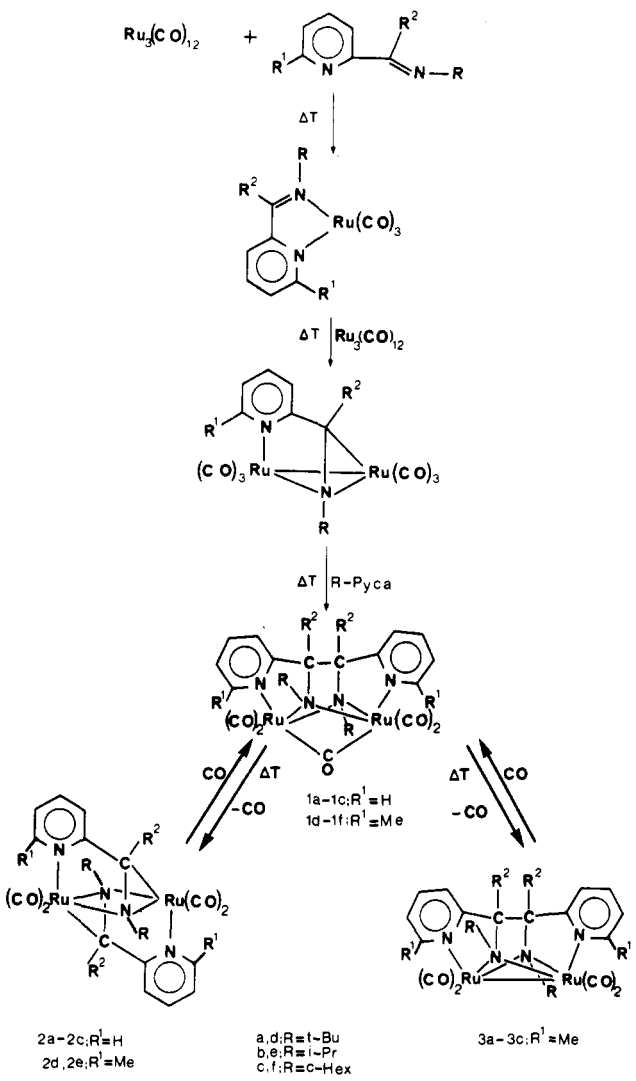

[a] R^2 = H in all cases.

tolyl-DAB, which proceeded directly to $Ru_2(CO)_4$(*p*-tolyl-DAB)$_2$. Surprisingly, in the case of *p*-tolyl-Pyca, formation of $Ru_2(CO)_4$(*p*-tolyl-Pyca)$_2$ could not be detected. Even at lower temperatures (80–90 °C), a complex mixture of unidentified compounds was obtained.

Upon prolonged heating of either pure $Ru_2(CO)_5$(R-APE) (**1a–c**) or a mixture of $Ru_3(CO)_{12}$ with R-Pyca in xylene at reflux, compounds of the stoichiometry $Ru_2(CO)_4$(R-Pyca)$_2$ (**2a–c**) were formed, as was inferred from their elemental analysis, FD-mass spectrometric data, IR ν(CO) data (Table IV), and, for $Ru_2(CO)_4$(*i*-Pr-Pyca)$_2$ (**2b**), X-ray structural analysis. The ^{1}H and ^{13}C NMR data (Tables V and VI) were in agreement with the assignment that the proposed structure (see Figure 2) is retained in solution. Thus, it appears that heating of $Ru_2(CO)_5$(R-APE) results in net loss of a CO molecule and the selective rupture of a carbon–carbon bond.

When the compounds $Ru_2(CO)_5$(R-APE{Me,H}) (**1d–f**) bearing a methyl group at the 6-position of both pyridine rings of the APE ligand were heated at ca. 140 °C for 8–16 hrs, new complexes of the stoichiometry $Ru_2(CO)_4$(R-APE{Me,H}) (**3a–d**) could be isolated. Their composition could be established from the combined analytical and spectrometric data (Tables IV–VI) of these complexes. The crude reaction mixture from which the $Ru_2(CO)_4$(R-APE{Me,H}) complexes were obtained contained small amounts of $Ru_2(CO)_4$(R-Pyca{Me,H})$_2$ (a product where carbon–carbon bond rupture has occurred), notably in case of R = *t*-Bu (**1d** → **3a** + **2d**). When the reaction mixture of $Ru_3(CO)_{12}$ and *t*-Bu-Pyca{Me,H} in xylene was refluxed for prolonged periods (20 h instead of 8 h), larger amounts (up to 40 rel %) of $Ru_2(CO)_4$(*t*-Bu-Pyca{Me,H})$_2$ (**2d**) were obtained. In case of R = *i*-Pr, viz., refluxing xylene solutions of either pure $Ru_2(CO)_5$(*i*-Pr-APE{Me,H}) or $Ru_3(CO)_{12}$ with *i*-Pr-Pyca{Me,H} for 70 h, only very little (10 rel %) of the $Ru_2(CO)_4$(*i*-Pr-Pyca{Me,H})$_2$ (**2e**) was present, besides $Ru_2(CO)_5$(*i*-Pr-APE{Me,H}) (**2b**). In these cases, the reactions were accompanied by extensive decomposition, which indicates that $Ru_2(CO)_n$(R-APE{Me,H}) (n = 4, 5), bearing methyl groups at the 6-position of the pyridine rings of the APE ligand, is very reluctant to give products that arise from carbon–carbon bond rupture in the APE ligand.

The described transformations of $Ru_2(CO)_5$(R-APE{R^1,R^2}) into $Ru_2(CO)_4$(R-APE{Me,H}) and $Ru_2(CO)_4$(R-Pyca)$_2$ for R^1 = Me and H, respectively, have also been observed for the related $Ru_2(CO)_n$(R-IAE) complexes. In these instances, either $Ru_3(CO)_{12}$ with R-DAB or pure $Ru_2(CO)_5$(R-IAE) could be converted into $Ru_2(CO)_4$(R-IAE), and this compound could be isolated in all cases except for R = *p*-tolyl. Prolonged heating of the R-IAE complexes in xylene eventually provided the C–C decoupled products $Ru_2(CO)_4$(R-DAB)$_2$ in good yield.[1] In the case of *p*-tolyl-DAB, the latter complex was formed directly; no intermediate $Ru_2(CO)_4$(*p*-tolyl-IAE) could be detected. This finding parallels the phenomena observed in the presently studied $Ru_2(CO)_n$(R-APE) complexes, where likewise no intermediate $Ru_2(CO)_4$(R-APE) could be detected; the conversion proceeded directly toward $Ru_2(CO)_4$(R-Pyca)$_2$ instead. Apparently, either $Ru_2(CO)_4$(R-APE) is not an intermediate in the C–C decoupling reaction leading to $Ru_2(CO)_4$(R-Pyca)$_2$, or it is not stable enough under the conditions required for the removal of one CO group from $Ru_2(CO)_5$(R-APE).

The behavior of the $Ru_2(CO)_n$(R-APE{Me,H}) (n = 4, 5) complexes (in which the pyridine moieties are substituted at the 6-position) is in sharp contrast to that of the unsubstituted compounds discussed above. Here, $Ru_2(CO)_4$(R-APE{Me,H}) was isolated as the major or only product, which subsequently could be converted into the C–C decoupled products $Ru_2(CO)_4$(R-Pyca{Me,H})$_2$, but only in very low yields. In the case of the *t*-Bu-Pyca{Me,H} ligand, slightly more (20–30%) of $Ru_2(CO)_4$(*t*-Bu-Pyca{Me,H})$_2$ could be isolated if we treated $Ru_3(CO)_{12}$ and excess *t*-Bu-Pyca{Me,H} directly in xylene at 140 °C, instead of following the route via $Ru_2(CO)_5$(*t*-Bu-APE{Me,H}). This result indicates that a second reaction pathway, leading directly from $Ru_2(CO)_6$(*t*-Bu-Pyca{Me,H}) to $Ru_2(CO)_4$(*t*-Bu-Pyca{Me,H})$_2$, may play a role, too (Scheme II). Possible mechanisms, explaining these observations will be discussed below.

CO-Induced C–C Coupling. When CO gas was bubbled through toluene solutions of either $Ru_2(CO)_4$(*i*-Pr-APE{Me,H}) (**3b**) or $Ru_2(CO)_4$(*i*-Pr-Pyca)$_2$ (**2b**) at 100 °C or when **3b** or **2b** was heated at 60 °C under 20 bars of CO pressure, a smooth regeneration of the complex $Ru_2(CO)_5$(*i*-Pr-APE{R^1,R^2}) (**1b,e**) was accomplished. After their isolation, these compounds could be decarbonylated again as described before (see Experimental Section). The interconversion between $Ru_2(CO)_n$(R-APE{Me,H}) (n = 4, 5) species merely consists of the sequential addition and elimination of the bridging CO ligand with concomitant rupture and formation, respectively, of the Ru–Ru bond. In the case of $Ru_2(CO)_4$(R-Pyca)$_2$ (**2b**), a reversible CO-induced carbon–carbon formation reaction between the imine carbon atoms C(1) of the ligands pertains. To the

best of our knowledge, such a CO-induced reductive coupling of two carbon centers is unprecedented. Carbon–carbon bond formation between σ-N, μ_2-N′, η^2-C=N′ bonded R-DAB ligands in dinuclear metal carbonyl complexes with (excess) ligands like R-DAB, electron-deficient alkynes, heteroallenes, etc. is known.[12] Furthermore, carbon–carbon bond formation in the presence of CO has been observed in the reaction of mononuclear iron complexes $Fe(CO)_3L$ (L = R-DAB, R-Pyca{H,R^2}) with electron-deficient alkynes.[14] These C–C coupling reactions, however, are not CO-induced; they also proceed in the absence of additional ligands. In several cases, insertion of a CO molecule in the M–N bond instead of the M–C bond of $M_m(CO)_n$(R-DAB) complexes has been observed,[14,15] whereas normally insertion of a CO molecule in M–C bonds to form an acyl fragment occurs.[16] In the present case, interestingly, the required CO molecule essentially triggers the carbon–carbon bond formation between two coordinated R-Pyca molecules in $Ru_2(CO)_4$(R-Pyca)$_2$.

The described CO-induced C–C coupling reaction has also been attempted for the analogous R-DAB system under similar conditions. In this case, however, no conversion of $Ru_2(CO)_4$(R-DAB)$_2$ into $Ru_2(CO)_5$(R-IAE) could be affected.[17]

IR Data (ν(CO) Region). The complexes $Ru_2(CO)_5$(R-APE{R^1,R^2}) display a characteristic pattern of four signals in the CO region (see Table IV), three of which appear between 1930 and 2020 cm^{-1} and one at about 1700 cm^{-1}. The later signal indicates the presence of a bridging CO group in the compounds. The complexes $Ru_2(CO)_4$(R-APE{R^1,R^2}) show the expected pattern of three ν(CO) signals, whereas the more symmetrical compound $Ru_2(CO)_4$(R-Pyca{R^1,R^2})$_2$ gives rise to only two ν(CO)'s (Table IV). These data are almost identical with those of the corresponding R-IAE and R-DAB analogues[1] which imply that neither the change of the organic ligand from R-IAE to R-APE nor the presence of a methyl substituent at the 6-position of the pyridine ring has a significant effect on the carbonyl frequencies of these compounds.

^{1}H NMR Data. The NMR data of the various complexes are listed in Tables V and VI; for those of the free R-Pyca{R^1,R^2} ligands, see ref 8. In the case of $Ru_2(CO)_4$(R-Pyca)$_2$ the signal of the imino protons N–C(H), which is a singlet due to the chemical equivalence of both R-Pyca's, is found in the range of 4.8–5.1 ppm. Its position has shifted about 3.5 ppm upfield relative to the chemical shift of the N=C(H) protons in the free R-Pyca ligands, consistent with a decreased paramagnetic contribution to the chemical shift, which is expected upon η^2-coordination of the N=C(H) moiety to Ru. The resonance positions of the N–C(H) signals in $Ru_2(CO)_4$(R-Pyca)$_2$ are found approximately 1 ppm downfield from those of the corresponding $Ru_2(CO)_4$(R-DAB)$_2$ complexes R = *i*-Pr, c-Hex). Compared to $Ru_2(CO)_6$(R-Pyca), the N=C(H) resonances of $Ru_2(CO)_4$(R-Pyca)$_2$ occur at 0.2 ppm downfield positions. The observation that the ^{1}H NMR signal of the imine protons of the η^2-coordinated N=C(H) moieties occur at lower field in the case of $Ru_2(CO)_4L_2$ compared to that of $Ru_2(CO)_6L$ has also been made for the analogous complexes where L = R-DAB.[1] Apparently, there is slightly more back-bonding from d orbitals on the Ru atoms to the π* levels of the N=C(H) moieties in $Ru_2(CO)_6L$ than in the case of $Ru_2(CO)_4L_2$ (L = R-DAB, R-Pyca). This seems to be consistent with more efficient charge relay through more π-back-bonding facilities in the former complex because of the higher number of π-accepting ligands.

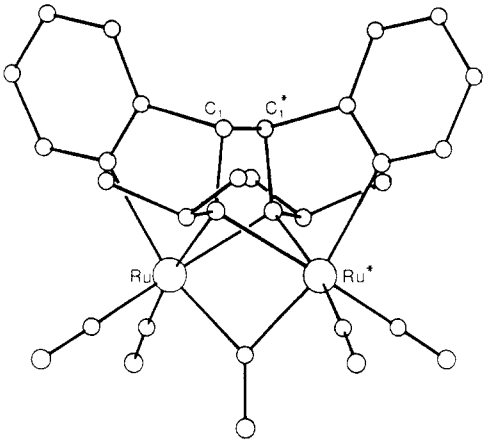

Figure 4. PLUTO representation of the molecular structure of $Ru_2(CO)_5$(*i*-Pr-APE) (**1b**).

In the complexes $Ru_2(CO)_n$(R-APE{R^1,R^2}) (n = 4, 5), the coupled N–C(H)C(H)–N carbon atoms (C(1) and C(1)* in Figure 4) are chiral. The geometric constraints imply that these carbon–carbon coupled compounds are formed in only one enantiomeric pair ((*R*,*R*) and (*S*,*S*)) of diastereomers. Indeed, their ^{1}H NMR spectra show only one resonance pattern. The resonances of the amido N–C(H)C(H)–N protons are found in the range 3.8–4.1 ppm (Table V), which is comparable to the range of 3.4–3.8 ppm observed for the related $Ru_2(CO)_n$(R-IAE) (*n* = 4, 5) complexes.[1] The chemical shift values of the N–C(H)C(H)–N protons in $Ru_2(CO)_n$(R-APE{R^1,R^2}) (*n* = 4, 5) are about 1 ppm lower than those for the N=C(H) protons in $Ru_2(CO)_4$(R-Pyca{R^1,R^2})$_2$ (Table V). This upfield shift in going from $Ru_2(CO_4$(R-Pyca)$_2$ to $Ru_2(CO)_n$(R-APE) (*n* = 4, 5) may be explained by regarding the relevant hydrogen atoms as attached to an η^2-coordinated imino carbon atom (in between sp^2 and sp^3) in the case of the former and as pure methine protons attached to an sp^3-hybridized carbon atom in the case of the latter complexes.

We note the diastereotopic nature of the methyl groups of the isopropyl derivatives **1b**, **1e**, **2b**, **2e**, and **3b**, which is very pronounced in the ^{1}H NMR of $Ru_2(CO)_4$(*i*-Pr-Pyca{R^1,R^2})$_2$ (**2b**, R^1, R^2 = H, H; **2e**, R^1, R^2 = Me, H). In these cases, the extreme high-field shift of the signal for one of the diastereotopic methyl groups, resonating at 0.1 ppm, points to the proximity of the metal atom (cf. Table V).

Temperature-dependent ^{1}H NMR (250-MHz) spectra of $Ru_2(CO)_5$(*t*-Bu-APE{R^1,R^2}) showed characteristic changes, i.e. broadening of the singlet due to the protons of the *t*-Bu groups at temperatures below +30 (R^1 = Me) or +60 °C (R^1 = H) and separation into three broad signals, which sharpened to give three single lines at −40 °C. This observation points to hindered rotation of the *t*-Bu group around the Me_3C–N bond in $Ru_2(CO)_5$(*t*-Bu-APE{R^1,R^2}), which could be frozen out at −40 °C. In the case of R = *i*-Pr this phenomenon could not be measured on the NMR time scale, even at −85 °C.

^{13}C NMR Data. The ^{13}C NMR data are in accord with the general structures of complexes **1a–f** and **3a–c**. Unfortunately, the compounds $Ru_2(CO)_4$(R-Pyca)$_2$ (**2a–e**) appeared to be insufficiently soluble to obtain ^{13}C NMR spectra. As above, the ^{13}C{^{1}H} spectra of $Ru_2(CO)_5$(R-

(14) Frühauf, H.-W.; Seils, F.; Goddard, R. J.; Romao, M. J. *Organometallics* **1985**, *4*, 948.
(15) Muller, F.; van Koten, G.; Vrieze, K.; Krijnen, B.; Stam, C. H. *J. Chem. Soc., Chem. Commun.* **1986**, 150.
(16) (a) Wojcicki, A. *Adv. Organomet. Chem.* **1973**, *11*, 33. (b) Calderazzo, F. *Angew. Chem., Int. Ed. Engl.* **1977**, *89*, 299.
(17) Keijsper, J.; Polm, L. H.; Muller, F., unpublished results.

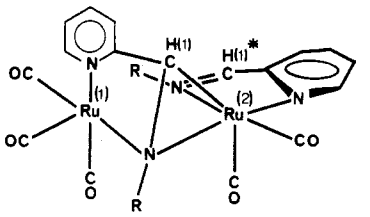

Figure 5. Asymmetric $Ru_2(CO)_5(R\text{-}Pyca)_2$ species.

APE{R^1,R^2}) show only single resonances, in line with the presence of only one enantiomeric pair of diastereomers. The resonance positions for the carbon atoms C(1) and C(1)* (see Figure 4) have shifted upfield relative to those in the free ligands (157–160 ppm), to δ values between 61 and 75 ppm, which is within the characteristic region for sp^3 C–N. This upfield shift of 80–90 ppm is somewhat smaller than the 95–100 ppm upfield shift for the C=N ^{13}C resonance in $Ru_2(CO)_6$(R-Pyca{R^1,R^2}) with respect to the free R-Pyca.[8] Two effects play a role: (i) an upfield shift due to the sp^3 hybridization of the coupled carbon atoms C(1)–C(1)* in $Ru_2(CO)_5$(R-APE{R^1,R^2}) and (ii) a downfield shift due to α-substitution by the coupling of carbon atom C(1) to C(1)*. Also, the more remote position of C(1) relative to the ruthenium atoms in $Ru_2(CO)_5$(R-APE{R^1,R^2}) compared to $Ru_2(CO)_6$(R-Pyca{R,$^1R^2$}) may have an as yet unknown influence on the chemical shift of C(1).

High-Temperature FT-IR Spectra. The thermal conversion of $Ru_2(CO)_5$(*i*-Pr-APE) in xylene at 120 °C was followed by FT-IR spectroscopy. The formation of two different products was observed in the FT-IR spectra depending on whether the reaction was studied in an open or a closed system. These cases will be discussed separately.

Open System. Upon heating of $Ru_2(CO)_5$(*i*-Pr-APE) in xylene in an open system, the original four bands in the ν(CO) region disappear and two intensive bands arise at 1912 and 1978 cm^{-1}, indicating that $Ru_2(CO)_4$(*i*-Pr-Pyca)$_2$ has been formed after loss of a CO molecule.

Closed System. At temperatures above 110 °C the IR absorption band arising from the bridging CO in the starting compound disappears while the terminal CO stretching vibrations shift toward higher wavenumbers. New bands appear at 2053 (s), 2036/2029 (m), 2001 (s), and 1976/1968 (m) cm^{-1}, which are retained upon lowering the temperature, indicating that an irreversible conversion has taken place. The new ν(CO) pattern, which is comparable to that observed in $Ru_2(CO)_5$(AIB)(alkyne),[18] points to the formation of an asymmetric $Ru_2(CO)_5$(R-Pyca)$_2$ species (see Figure 5), in which one Ru atom bears two and the other Ru bears three terminal CO groups.

It has been established that Ru_2CO_5AIB(alkyne) has five terminal CO groups, grouped as indicated above; only there, due to the presence of the electron-withdrawing alkyne ligand MeOOCC≡CCOOMe, the strong bands are shifted toward higher frequencies (2085 and 2016 cm^{-1}) relative to the presently studied asymmetric $Ru_2(CO)_5$(R-Pyca)$_2$ complex.

The proposed structure of the complex (see Figure 5) can exist in two stereoisomeric forms, which only differ in their geometries around the Ru atoms. The stereoisomerism of this molecule may account for the splitting observed in the 2036/2029 and 1976/1968 cm^{-1} bands. Also, the proposed structure accounts for the hypsochromic shift of all five ν(CO) frequencies in this intermediate, compared to that of the parent compound $Ru_2(CO)_5$(R-APE).[19] Furthermore, the intermediacy of such a species (which is unstable under the applied reaction conditions but is apparently stable in a closed IR cell)[20] may explain the different chemical behavior that has been observed for the $Ru_2(CO)_n$(R-APE) and $Ru_2(CO)_n$(R-APE{Me,H}) compounds. This will be discussed below, under "Formation of $Ru_2(CO)_4$(R-Pyca)$_2$ and $Ru_2(CO)_4$(R-Pyca{Me,H})$_2$".

Mechanistic Aspects. Formation of $Ru_2(CO)_5$(R-APE{R^1,R^2}). Complexes of ruthenium containing C–C coupled products of R-DAB and unsaturated ligands are known[12,21] and are reported now also for R-Pyca analogues starting from $Ru_2(CO)_6$(R-Pyca{R^1,R^2}) and a R-Pyca ligand. The basic structural features of the complexes $Ru_2(CO)_5$(R-APE{R^1,R^2}) that arise are comparable to species $Ru_2(CO)_5$L (L = R-IAE, R-AIB, etc.) derived from reactions of $Ru_2(CO)_6$(R-DAB) with R-DAB, a heteroallene, or an alkyne, respectively.[1,18,21] This type of compounds exhibits basically a [{Ru(CO)$_2$}$_2$(μ-CO)] core, which is doubly bridged by a N–C–C–X moiety (X = N, C, S). In all cases, the formerly η^2-coordinated α-imine group in $Ru_2(CO)_6$(R-DAB) is overall reductively coupled to an unsaturated C=X function in the incoming ligand. Compounds such as $Ru_2(CO)_5$L (L = R-APE, R-IAE, etc.) can therefore be viewed as insertion products of an unsaturated system into a Ru–C bond.

The formation of $Ru_2(CO)_5$(R-APE{R^1,R^2}) and $Ru_2(CO)_4$(R-Pyca{R^1,R^2})$_2$ from $Ru_2(CO)_6$(R-Pyca{R^1,R^2}) and R-Pyca{R^1,R^2} cannot occur by a reaction sequence as has been outlined for similar reactions of the R-DAB/R-IAE analogues (Scheme I),[4,12,22] since the intermediate formation of an 8e donor bonding of an R-Pyca ligand would involve the participation of the C=N moiety of the pyridine ring, which is unfavorable because this would require loss of aromatic resonance stabilization. In the case of $Ru_2(CO)_6$(R-Pyca{R^1,R^2}) coupling with another R-Pyca molecule may take place, either by substitution of a CO molecule by a second R-Pyca molecule or by initial C–C coupling of the η^2-coordinated N=C unit and the N=C unit of the incoming R-Pyca. The latter possibility has direct analogy in the direct insertion of small molecules like acetylenes, carbodiimides, etc. into the η^2-N=C unit of $Ru_2(CO)_6$(R-DAB) complexes.[4,12,21] The first alternative possibility seems less likely, since the geometry of the coordination sites of Ru would force a second R-Pyca ligand into a noninteractive position relative to the η^2-coordinated N=C moiety.

The coupling according to the second possibility may take place by a polar mechanism, in which the carbon atom of the η^2-coordinated imine group acts as the nucleophile

(18) Staal, L. H.; van Koten, G.; Vrieze, K.; van Santen, B. F. K.; Stam, C. H. *Inorg. Chem.* **1981**, *20*, 3598. AIB stands for *N*-(alkylamino)-*N*-(alkylimino)butenyl and is formed from C–C coupling of R-DAB with an activated alkyne.

(19) In the asymmetric compound (Figure 5) back-donation from Ru-(1) is now to three terminal CO's instead of two terminal and one bridging CO in $Ru_2(CO)_5$(R-APE). Consequently, the ν(CO) of these three CO's all shift toward higher wavenumbers. Ru(2) has back-bonding facilities to an η^2-C=N function of one R-Pyca ligand and to two terminal CO's in the asymmetric complex, which is more efficient than to two terminal and one bridging CO in the parent molecule. Hence, also the signals of the terminal CO's at Ru(2) will shift hypsochromically.

(20) All our efforts to isolate the proposed, asymmetric intermediate have been unsuccessful. An experiment comparable to that in the IR cell on a larger scale in a Schlenk tube, which was *completely* filled with either a neat xylene solution or a CO-saturated xylene solution of $Ru_2(CO)_5$(*i*-Pr-APE), yielded, after heating at several temperatures and subsequent cooling and opening of the tube, only $Ru_2(CO)_4$(*i*-Pr-Pyca)$_2$ and $Ru_2(CO)_5$(*i*-Pr-APE). Possibly, the asymmetric intermediate is formed initially but readily looses CO upon the opening of the reaction vessel.

(21) Keijsper, J.; Polm; L. H.; van Koten, G.; Vrieze, K.; Schagen, J. D.; Stam, C. H. *Inorg. Chim. Acta* **1985**, *103*, 137.

(22) Keijsper, J.; Polm, L. H.; van Koten, G.; Vrieze, K.; Seignette, P. F. A. B.; Stam, C. H. *Inorg. Chem.* **1985**, *24*, 518.

attacking the slightly positively polarized carbon atom of the free imine function of the R-Pyca molecule. The nucleophilic character of the carbon atom of the η^2-coordinated N=C moiety in $Ru_2(CO)_6$(R-Pyca) may be envisaged by accepting a reversal of the polarization of this imine fragment compared to that of a free imine. This reverse polarization becomes conceivable if one regards the η^2-bonding of the imine groups, i.e. donation of electron density from the π-orbital of the imine (located mainly on the nitrogen atom) to metal d orbitals, on the one hand, and back-donation of Ru to the imine π^*-orbital (which is largely localized on the carbon atom) building up electron density at the carbon, on the other hand.

After the C–C bond formation has taken place, a CO is expelled by attack of the pyridine nitrogen atom of the incoming ligand on Ru. The molecule rearranges by formation of a second μ_2-N bridge and a CO bridge, to yield $Ru_2(CO)_5$(R-APE{R^1,R^2}).

Formation of $Ru_2(CO)_4$(R-Pyca)$_2$ and $Ru_2(CO)_4$(R-APE{Me,H}). In $Ru_2(CO)_5$(R-APE{R^1,R^2}) a 10e donating R-APE{R^1,R^2} ligand stabilizes the $Ru_2(CO)_5$ core. When one CO is evolved from this compound, the product will be electronically unsaturated and either formation of a metal–metal bond or formation of two 6e donating ligands will be necessary in order to yield a stable complex. The latter mode of reaction requires the breaking of the C(1)–C(1)* bond (Figure 4) in the R-APE ligand into two R-Pyca ligands. In view of the high-temperature FT-IR spectra it seems that in the thermal conversion of $Ru_2(CO)_5$(R-APE) an asymmetrically substituted species, $Ru_2(CO)_5$(R-Pyca)$_2$ (Figure 5), with five terminal CO groups is involved. Such a species may arise from $Ru_2(CO)_5$(R-APE) via thermally induced carbon–carbon bond cleavage, initiated by the twisting of the ligand system. If now the $Ru(CO)_2L$ and $Ru(CO)_3L$ moieties rotate with respect to each other, the $Ru_2(CO)_4$(R-Pyca)$_2$ is formed after loss of one terminal CO from the $Ru(CO)_3L$ fragment, which is induced by formation of an η^2-C=N bond to Ru(1). This sequence could explain that carbon–carbon decoupling does only sluggishly occur in the case of the 6-Me-substituted R-APE analogue $Ru_2(CO)_5$(R-APE{Me,H}), since in that case the existence of an asymmetric species as depicted in Figure 5 is less likely, as it will be destabilized by substantial internal steric hindrance. From a study of models of the asymmetric $Ru_2(CO)_5$(R-Pyca{Me,H})$_2$, with a CH_3 group at the pyridine 6-position, it appears that steric interference of this pyridine methyl substituent with the equatorial terminal CO groups of the $Ru(CO)_3L$ and $Ru(CO)_2L$ fragments would result. Hence, such an intermediate will be formed only reluctantly. In that case, direct elimination of the bridging CO in the parent $Ru_2(CO)_5$(R-APE{Me,H}) becomes competitive, leaving two Ru-centered radicals which form a metal–metal bond at a very fast rate. Once this Ru–Ru bond is formed, the $Ru_2(CO)_4$(R-APE{Me,H}) molecule is apparently stable with regard to stereoisomerization into $Ru_2(CO)_4$(R-Pyca{Me,H})$_2$. The fact that yet minor amounts of $Ru_2(CO)_4$(R-Pyca{Me,H})$_2$ are found in some reactions mixtures must at least partly be accounted for by assuming a competitive route, as has already been discussed under "Syntheses" (vide supra). Furthermore, small amounts of $Ru_2(CO)_4$(R-Pyca{Me,H})$_2$ may be formed from $Ru_2(CO)_5$(R-APE{Me,H}) by the route delineated above for the corresponding 6-unsubstituted pyridine analogues because the steric hindrance will retard but not completely inhibit the described reaction pathway. The fact that in this case, however, substantial amounts of decomposition products were observed means that the route from $Ru_2(CO)_5$(R-APE{Me,H}) to $Ru_2(CO)_4$(R-Pyca{Me,H})$_2$ is highly unfavorable.

CO-Induced Carbon–Carbon Bond Formation. The CO-induced C–C bond formation, from $Ru_2(CO)_4$(R-Pyca)$_2$ to give $Ru_2(CO)_5$(R-APE), most likely takes the same pathway in the opposite direction as the C–C decoupling reaction outlined above. Thus, one η^2-C=N bond of either of the two coordinated R-Pyca's in $Ru_2(CO)_4$(R-Pyca)$_2$ is ruptured, allowing a CO to take the vacant coordination site, which yields the asymmetric $Ru_2(CO)_5$(R-Pyca)$_2$ species as depicted in Figure 5. In the presence of excess CO the equilibrium $Ru_2(CO)_4$(R-Pyca)$_2$ + CO $\rightleftharpoons$ $Ru_2(CO)_5$(R-Pyca)$_2$ will be shifted to the right, so that intramolecular C–C coupling between C(1) and C(1)* can occur to give the stable $Ru_2(CO)_5$(R-APE) compound.

Conclusions

It has been shown that C–C bond formation between an η^2-coordinated imine group and a free imine group is not restricted to R-DAB but can also occur in case of R-Pyca derivatives. Whereas thermal reactions of $Ru_2(CO)_5$(R-IAE) species irreversibly yield $Ru_2(CO)_4$(R-DAB)$_2$, such a carbon–carbon bond rupture reaction appears to be reversible for several R-Pyca analogues in the presence of CO. The scope of this type of building of organic fragments on bimetallic species can probably be enlarged by studying the reactions of other unsaturated molecules with $Ru_2(CO)_6$(R-Pyca).

Acknowledgment. We wish to thank Mr. D. Heijdenrijk for collecting the X-ray data, Mr. R. H. Fokkens for recording the mass spectra, Mr. G. S. Schoemaker for assistance during the FT-IR experiments, Mr. F. Muller and Mr. Ch. Mahabiersing for performing several experiments, and Dr. H.-W. Frühauf for critically reading the manuscript. One of the reviewers is thanked for several comments regarding the crystal structure.

Registry No. **1a**, 107148-58-3; **1b**, 107148-59-4; **1c**, 107148-60-7; **1d**, 107148-61-8; **1e**, 107148-62-9; **1f**, 107148-62-9; **2a**, 107148-73-2; **2b**, 107148-74-3; **2c**, 107148-75-4; **2d**, 107148-76-5; **2e**, 107173-88-6; **3a**, 107148-64-1; **3b**, 107148-65-2; **3c**, 107148-66-3; $Ru_3(CO)_{12}$, 15243-33-1; $Ru_2(CO)_6$(*t*-Bu-Pyca), 107148-67-4; $Ru_2NCO)_6$(*i*-Pr-Pyca), 107148-68-5; $Ru_2(CO)_6$(c-Hex-Pyca), 107148-69-6; $Ru_2(CO)_6$(*t*-Bu-Pyca(Me,H)), 107148-70-9; $Ru_2(CO)_6$(*i*-Pr-Pyca(Me,H)), 107148-71-0; $Ru_2(CO)_6$(c-Hex-Pyca(Me,H), 107148-72-1; *t*-Bu-Pyca, 21478-42-2; *i*-Pr-Pyca, 7032-23-7; c-Hex-Pyca, 7166-35-0; *t*-Bu-APE, 107148-77-6; *i*-Pr-APE, 107148-78-7; c-Hex-APE, 107148-79-8; *i*-Pr-APE(Me,H), 107148-80-1; *t*-Bu-Pyca(Me,H), 107148-81-2; *i*-Pr-Pyca(Me,H), 78004-29-2; c-Hex-Pyca(Me,H), 107148-82-3; C, 7440-44-0; Ru, 7440-18-8.

Supplementary Material Available: Listings of analytical data, anisotropic thermal parameters, and all bond distances and angles (7 pages); a listing of observed and calculated structure factors (7 pages). Ordering information is given on any current masthead page.